



## EFFECTS OF ANNEALING TEMPERATURE ON STRUCTURAL, MORPHOLOGY AND OPTICAL PROPERTIES OF TiO<sub>2</sub> THIN FILM

N. D. Mohd Said<sup>1,2</sup>, M. Z. Sahdan<sup>1</sup>, I. Senain<sup>1</sup>, A. S. Bakri<sup>1</sup>, S. A. Abdullah<sup>1</sup>, F. Mokhter<sup>1</sup>, A. Ahmad<sup>1</sup> and H. Saim<sup>1</sup>

<sup>1</sup>Microelectronics & Nanotechnology-Shamsuddin Research Centre, Universiti Tun Hussein Onn Malaysia, Batu Pahat, Johor, Malaysia

<sup>2</sup>Department of Electrical Engineering, Politeknik Merlimau, Pejabat Pos Merlimau, Merlimau, Melaka, Malaysia

E-Mail: [zainizan@gmail.com](mailto:zainizan@gmail.com)

### ABSTRACT

This paper reports on the effects of Titanium dioxide (TiO<sub>2</sub>) thin films which were deposited by sol-gel spin coating technique with different annealing temperatures at 300°C, 400°C and 500°C for a period of 1 hour. The precursor used was 2 ml of Titanium (IV) Butoxide. The research is focusing more on the uniformity of TiO<sub>2</sub> thin films. TiO<sub>2</sub> films were characterized by structural properties, surface morphological, surface topological and optical properties. For 500°C annealed film, transparent TiO<sub>2</sub> thin film were deposited more uniform than the others. The surface morphologies of the TiO<sub>2</sub> thin film were observed by a field emission scanning electron microscope (FESEM). The surface topologies and roughness were characterized by an atomic force microscope (AFM). The structural properties were characterized by an X-ray diffractometer (XRD). The optical properties were characterized with an ultraviolet-visible spectrometer (UV-Vis). The results indicated the optical transmittance of TiO<sub>2</sub> thin films were elevated with higher annealing temperature.

**Keywords:** annealing temperature, titanium IV butoxide, anatase.

### INTRODUCTION

Titanium dioxide (TiO<sub>2</sub>) has good physical properties such as high dielectric constant, good mechanical resistance and good insulation properties [1]. TiO<sub>2</sub> is an n-type semiconductor with 3.2 eV band gap and has a range of utilization for the applications of photocatalytic [2], antireflection coatings [3], solar cells [4] and gas sensor [5]. The physical, optical and structural properties of titanium dioxide (TiO<sub>2</sub>) depend on crystalline phases of the material. TiO<sub>2</sub> is a material with three crystalline phases; anatase, rutile and brookite are commonly observed in this thin films [6]. Rutile is the most stable at all temperatures in very acidic or basic. In addition, it has high refractive index (2.5 ~ 4.5) [7], [8]. Stoichiometry of rutile TiO<sub>2</sub> is greatly dependent on parameters of deposition, particularly in condition of annealing and the environment. The melting point of rutile is 1850°C associated with purity titanium dioxide. Anatase and brookite are more stable at lower temperature, but both react to rutile at high temperatures (915°C to 750°C of anatase and brookite). Moreover, lower annealing temperature at lesser than 350°C, the structural of TiO<sub>2</sub> on thin film becomes amorphous [6], [9],[10].

TiO<sub>2</sub> thin films can be synthesized using various techniques, including sputtering [11], electrophoretic deposition [12], sol-gel [13],[14], dip coating [15] and spin coating [16]. Spin coating is extensively used in the fabricate of TiO<sub>2</sub> thin films due to fast growth, capacity for handling large sample size, mass production capacity and high yields. However, spin coating technique involves a process of subsequent annealing, which is known to increase the spread of impurities from the substrate of glass coating. This process tends to restrict the grain growth in the film and also increases the number of lattice defects, which decreases the photocatalytic activity of the TiO<sub>2</sub> thin films.

The intention of this work was the optimization process of Titanium (IV) Butoxide concentration to produce uniform and transparent TiO<sub>2</sub> thin films using sol-gel spin coating and to determine the optimum annealing temperature, which would produce the best performance of thin film.

### EXPERIMENTAL

Figure-1 indicates the research methodology of the optimization of TiO<sub>2</sub> thin film for solar cell application. The glass substrates were cleaned with acetone in an ultrasonic bath for 5 minutes at 50°C and purged to dry with nitrogen gas.

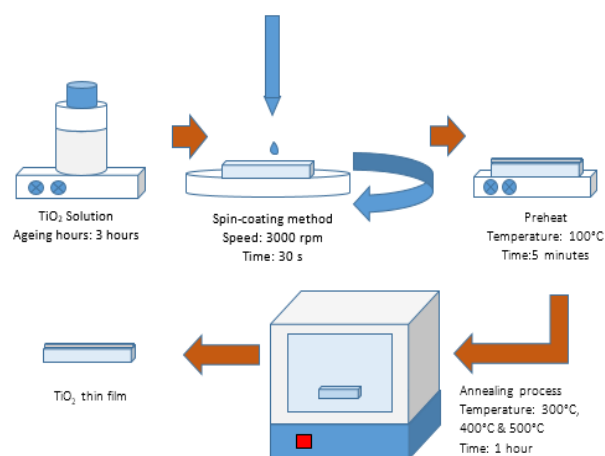


**Figure-1.** Schematic diagram of sol-gel process and deposition of TiO<sub>2</sub> thin film.

The starting materials used were titanium butoxide as precursor, ethanol as solvent, deionised water as a function of adding the oxygen (O), acids and triton X-



100 as a stabilizer to avoid precipitation in solution and at the same time used to increase the conductivity of films. The type of acids were glacial acetic acid and hydrochloric acid. For solution preparation, titanium butoxide mixed with ethanol, acid catalysts and triton X -100 were stirred for 3 hours for ageing process at room temperature.  $\text{TiO}_2$  solution used for the deposition of thin films by spin-coating method was obtained by the partial hydrolysis and condensation.

$\text{TiO}_2$  films were deposited by spin coating method (3000 r.p.m for 30s) for 5 layers.  $\text{TiO}_2$  solution was dropped up to 10 times onto the substrates. Each layer was preheated at  $100^\circ\text{C}$  for 5 minutes. The thin films were annealed at  $500^\circ\text{C}$  for 1 hour. Annealing also produces better physical attachment which improves the electronic contact between all the particles of the thin films. After annealing at  $500^\circ\text{C}$  for 1 hour, the thin films were underwent slow cooling at room temperature. Then, thin films were coated with gold electrode by using sputter coater. The sputter coater was set to 20mA for 30 seconds. Then,  $\text{TiO}_2$  thin films were physically characterized.

The surface morphology of the  $\text{TiO}_2$  thin film was observed by a field emission scanning electron microscope (FESEM). The magnification of the images is 50K times. The thickness of each sample was characterized using KL Tenko surface profiler. The optical transmittance spectra were recorded in the wavelength range of 300-1000nm using a Shimadzu Ultra Violet-Visible Spectrometer (UV-Vis). The structural properties were characterized by PANalytical Smartpowder X-ray diffractometer (XRD). XRD is used to identify the crystallinity and phases of the  $\text{TiO}_2$  film. The measurement was obtained at  $2\theta$  degree by  $\text{Cu K}\alpha$  radiation. The surface topologies and roughness were characterized by an Atomic Force Microscope (AFM),

XE-100 Park system at room temperature. With noncontact cantilever and non-contact mode, this characterization method promises a non-destructive testing. Other than that, it also capable to give the information on grain size and roughness of  $\text{TiO}_2$  thin film.

The estimation of the crystal grain size,  $D$  according to Scherrer's equation:

$$D = \frac{0.9\lambda}{\beta \cos \theta} \quad (1)$$

Where  $\lambda$  is the light wavelength,  $\beta$  is the full width half maximum and  $\theta$  is the degree of diffraction.

## RESULTS AND DISCUSSION

### Surface morphology

Figure-2 shows the cross-sectional view of  $\text{TiO}_2$  thin films annealed at  $500^\circ\text{C}$ . For sample deposited using 1.5 ml, 2.0 ml and 2.5 ml of Titanium (IV) Butoxide, the thicknesses are 41.3 nm, 88.1 nm and 98.4 nm, respectively. It shows the increasing of thickness when the concentration of Titanium (IV) Butoxide was increased. Figure-3 shows that 2ml of Titanium (IV) Butoxide, the  $\text{TiO}_2$  thin film is more uniformity than the others.

Figure-4 shows three types of sample that annealed at  $500^\circ\text{C}$ ,  $400^\circ\text{C}$  and  $300^\circ\text{C}$ . In this research, annealing of  $\text{TiO}_2$  thin film at  $500^\circ\text{C}$  shows the particles size between 15.9 nm to 49.1 nm. On the other hand, annealing at  $300^\circ\text{C}$  and  $400^\circ\text{C}$  had grown particles ranging from 12.7 nm to 14.0 nm and 14.1 nm to 15.5 nm. It was found that the particle size increases as the annealing temperature increased.

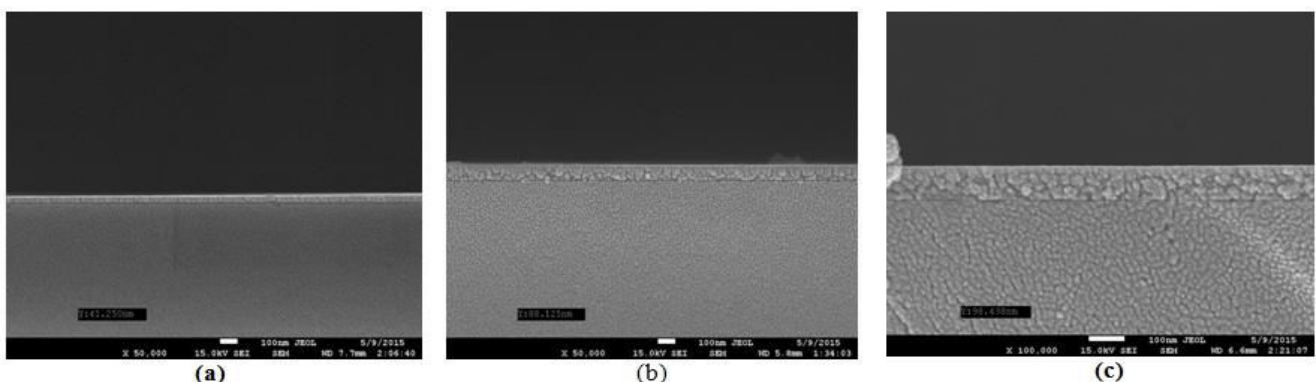
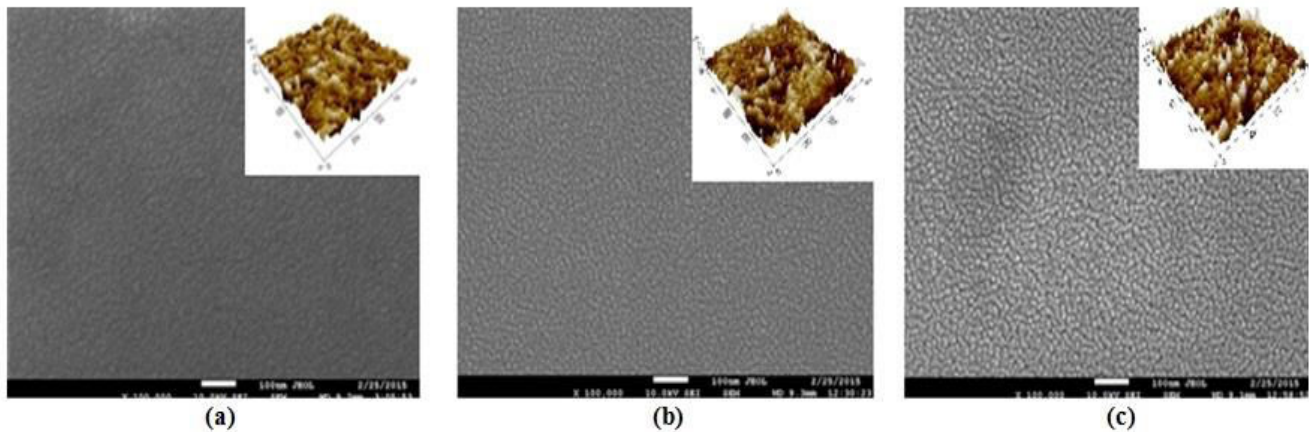


**Figure-2.** Cross section of  $\text{TiO}_2$  thin film for different titanium butoxide concentration (a) 1.5 ml (b) 2.0 ml and (c) 2.5 ml.

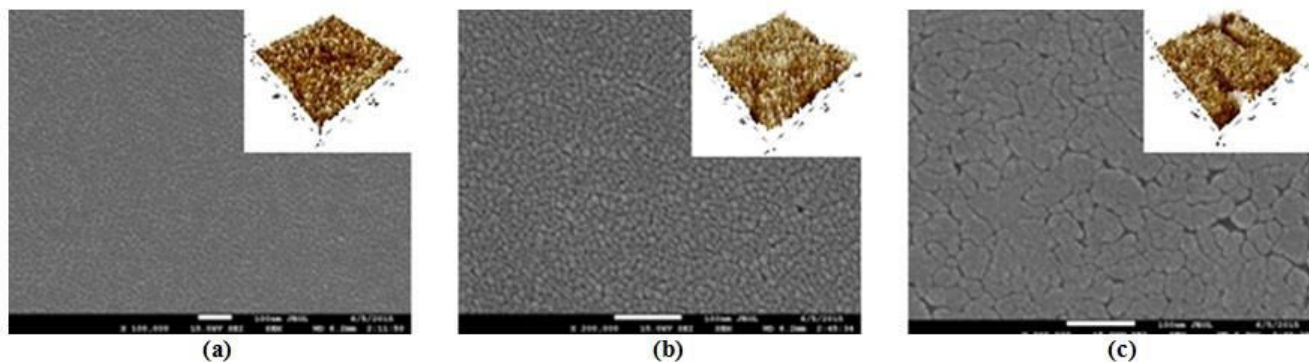
### Surface topology

Figure-4 shows two dimensional AFM images of the deposited films annealed at  $300^\circ\text{C}$ ,  $400^\circ\text{C}$  and  $500^\circ\text{C}$ . When the annealing temperature was increased, the grain size was decreased. The grain size for annealing temperature of  $300^\circ\text{C}$ ,  $400^\circ\text{C}$  and  $500^\circ\text{C}$  are 91 nm, 56 nm and 49 nm, respectively. Furthermore, the AFM roughness

analysis also presented the value of the roughness parameters. The lower roughness value represents good homogeneity of the  $\text{TiO}_2$  particles on the surface. AFM image at  $500^\circ\text{C}$  has the lowest roughness. Table-1 shows the grain size and surface roughness of  $\text{TiO}_2$  thin film. The average particle size lies in the range of nm, which is slightly larger than that obtained from the XRD results.



**Figure-3.** Surface morphology of  $\text{TiO}_2$  thin film for different titanium butoxide concentration (a) 1.5 ml (b) 2.0 ml and (c) 2.5 ml.



**Figure-4.** Surface morphology of  $\text{TiO}_2$  thin film for different annealing temperature (a) 300°C (b) 400°C and (c) 500°C.

**Table-1.** Grain size and surface roughness with different annealing temperature.

Annealing temperature	Grain size	Surface roughness
300°C	91 nm	0.383 nm
400°C	56 nm	0.811 nm
500°C	49 nm	1.349 nm

### Structural Properties

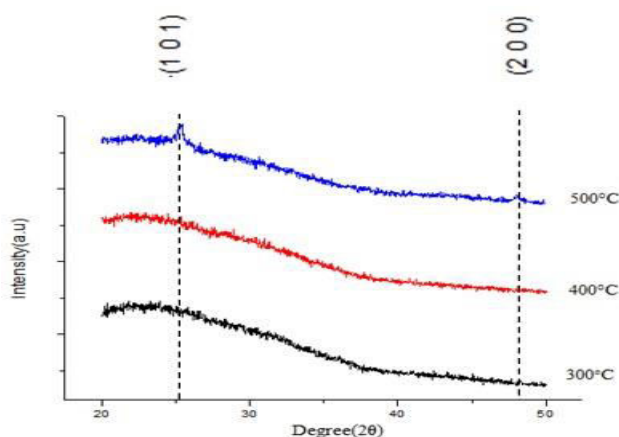


**Figure-5.** X-ray diffraction patterns of the  $\text{TiO}_2$  thin film at various annealing temperature.

XRD is essential in the determination of the crystallinity. Figure-5 shows the XRD spectra of the  $\text{TiO}_2$  thin films, as-deposited at different annealing temperature namely 300°C, 400°C and 500°C. As-deposited samples were basically polymorphs and characteristic peaks were visible corresponding to  $\text{TiO}_2$  which major anatase phase at 500°C. The thin film was in anatase crystalline state with a better orientation of (101) at 25.32°. Besides that, XRD peaks at 48.14° corresponded to the anatase orientation (200) peak also shown in the annealed samples which could be indexed as standard tetragonal stable anatase crystalline state. However at 300°C and 400°C, annealing temperature, no peaks were visible because of small size of the crystal and very low intensity of the diffracted X-rays. In anatase phase that the orientation (101) surface was the most stable and dominant peak with the highest intensity. The intensity of  $\text{TiO}_2$  thin film existed with annealing temperature. The weak intensity of diffraction peaks for the as-deposited film indicates the presence of amorphous phase.

The temperature dependence of XRD patterns can be described by the mobility of atomic species in thin films at various annealing temperature. At low annealing temperature, the evaporated species possess small energy and a low surface mobility causing a less controlled surface structure. The low mobility of atoms avoids full



crystallization of the films. Nevertheless, at high annealing temperature, and high temperature, atoms acquire high sufficient mobility to organize themselves in more crystalline arrangement.

### Optical properties

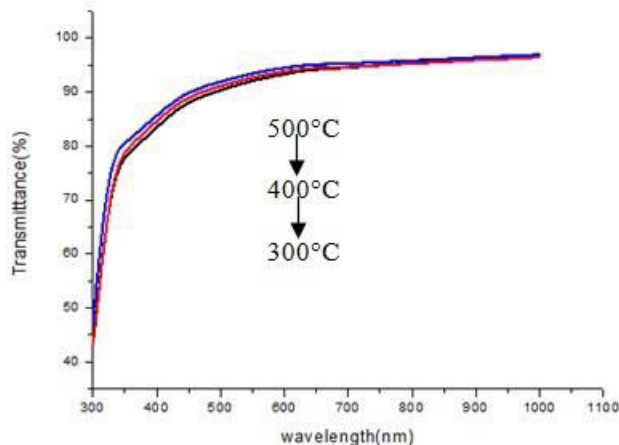


**Figure-6.** The transmittance spectra of TiO<sub>2</sub> thin films at different annealing temperature (a) 500°C (b) 400°C (c) 300°C.

Figure-6 shows the optical transmittance of the thin films annealed at 300°C, 400°C and 500°C in the spectra region of 300-1000 nm. Glasses were used as substrate in this experiment to prevent the influence of the absorption edge of substrate. Based on the figure, it shows a slight decrease in transmittance with the increasing of annealing temperature. The optimum TiO<sub>2</sub> thin films spectra exhibited high visible transmittance as high as 98% for annealing temperature of 500°C. The energy band gap is evaluated using Tauc's plot based on equations as the following:

$$E = \frac{hc}{\lambda} \quad (2)$$

and

$$\alpha = \frac{1}{d} \ln\left(\frac{1}{T}\right) \quad (3)$$

While  $h$ ,  $c$  and  $\lambda$  are plank constant ( $4.136 \times 10^{-15}$  eV), speed of light ( $3 \times 10^8$  ms<sup>-1</sup>) and wavelength, respectively. Where,  $d$  and  $T$  are the absorption coefficient, film's thickness and transmittance, respectively. Energy band gap normally refers to the energy difference (in electron volts) between the top of the valence band and the bottom of the conduction band in semiconductors. Conversely at the wavelength between 300nm-340nm, the film at 300°C initially shows the lowest transmittance and gradually increases. On the other hand film annealed at 500°C shows the highest transmittance at 1000 nm wavelength. Nevertheless, all samples exhibit more than 90% of transmittance in the visible light region.

The transmittance for all annealed samples rises with increasing wavelength.

### CONCLUSIONS

This paper presents the results of the optimization process to produce uniform and transparent TiO<sub>2</sub> thin films using sol-gel spin coating. TiO<sub>2</sub> thin films were more uniform using 2ml Titanium (IV) Butoxide. The surface morphology of the TiO<sub>2</sub> thin films were investigated using FESEM measurements. Transparent Titanium dioxide thin films that has been successfully annealed at 500°C. The samples were anatase phases and the particle size was in nanometer scale which is confirmed by XRD pattern analysis. The particle was measured using AFM at annealing temperature of 500°C and the smallest grain size is 49 nm. The surface roughness at 500°C is 1.349 nm. UV-vis spectra showed that the absorption edge of these films were at shorter wavelength. At 500°C the optimum transmittance was obtained which is 98% and sufficient for optoelectronic applications especially for solar cell.

### ACKNOWLEDGEMENTS

The authors would like to acknowledgement the Ministry of Education Malaysia for the financial support through FRGS grant vote 1210 and UTHM for the technical facilities.

### REFERENCES

- [1] C. H. Heo, S.-B. Lee, and J.-H. Boo, "Deposition of TiO<sub>2</sub> thin films using RF magnetron sputtering method and study of their surface characteristics," *Thin Solid Films*, vol. 475, no. 1–2, pp. 183–188, Mar. 2005.
- [2] K. Eufinger and D. Poelman, 'TiO<sub>2</sub> thin films for photocatalytic applications, vol. 661, no. 2. 2008.
- [3] R. C. Jayasinghe, A. G. U. Perera, H. Zhu, and Y. Zhao, "Optical properties of nanostructured TiO<sub>2</sub> thin films and their application as antireflection coatings on infrared detectors," vol. 37, no. 20, pp. 4302–4304, 2012.
- [4] D. Mahesh and J. Rajesh, "TiO<sub>2</sub> Microstructure , Fabrication of thin Film Solar Cells and Introduction to Dye Sensitized Solar Cells," vol. 2, no. 2012, pp. 25–29, 2013.
- [5] S. Boyadjiev, V. Georgieva, L. Vergov, Z. Baji, F. Gáber, and I. M. Szilágyi, "Gas sensing properties of very thin TiO<sub>2</sub> films prepared by atomic layer deposition (ALD)," *J. Phys. Conf. Ser.*, vol. 559, p. 012013, Nov. 2014.
- [6] A. N. Banerjee, "The design, fabrication, and photocatalytic utility of nanostructured semiconductors: focus on TiO<sub>2</sub>-based



nanostructures,” *Nanotechnol. Sci. Appl.*, vol. 4, pp. 35–65, Jan. 2011.

film,” *Phys. B Condens. Matter*, vol. 413, pp. 40–46, Mar. 2013.

- [7] W. Group, I. S. Name, and P. White, “1 . Exposure Data,” vol. 1988, no. October 1988, 1989.
- [8] D. a. H. Hanaor and C. C. Sorrell, “Review of the anatase to rutile phase transformation,” *J. Mater. Sci.*, vol. 46, no. 4, pp. 855–874, Dec. 2010.
- [9] M. Epifani, A. Helwig, J. Arbiol, R. Díaz, L. Francioso, P. Siciliano, G. Mueller, and J. R. Morante, “TiO<sub>2</sub> thin films from titanium butoxide: Synthesis, Pt addition, structural stability, microelectronic processing and gas-sensing properties,” *Sensors Actuators B Chem.*, vol. 130, no. 2, pp. 599–608, Mar. 2008.
- [10] P. Engineering and N. S. Wales, “Novel Uses of Titanium Dioxide for Silicon Solar Cells,” no. April, 2002.
- [11] M. M. A. El-raheem and A. M. Al-baradi, “Optical properties of as-deposited TiO<sub>2</sub> thin films prepared by DC sputtering technique,” vol. 8, no. 31, pp. 1570–1580, 2013.
- [12] A. K. Singh and U. T. Nakate, “TiO<sub>2</sub> Microwave Synthesis , Electrophoretic Deposition of Thin Film , and Photocatalytic Properties for Methylene Blue and Methyl Red Dyes,” vol. 2014, 2014.
- [13] S. Naghibi, S. Vahed, O. Torabi, A. Jamshidi, and M. H. Golabgir, “Exploring a new phenomenon in the bactericidal response of TiO<sub>2</sub> thin films by Fe doping: Exerting the antimicrobial activity even after stoppage of illumination,” *Appl. Surf. Sci.*, vol. 327, pp. 371–378, Feb. 2015.
- [14] D. V. Pinjari, K. Prasad, P. R. Gogate, S. T. Mhaske, and a B. Pandit, “Synthesis of titanium dioxide by ultrasound assisted sol-gel technique: effect of calcination and sonication time.,” *Ultrason. Sonochem.*, vol. 23, pp. 185–91, Mar. 2015.
- [15] Y. Hu and C. Yuan, “Low-temperature Preparation of Photocatalytic TiO<sub>2</sub> Thin Films on Polymer Substrates by Direct Deposition from Anatase Sol,” vol. 22, no. 2, pp. 239–244, 2006.
- [16] M. R. Golobostanfard and H. Abdizadeh, “Effects of acid catalyst type on structural, morphological, and optoelectrical properties of spin-coated TiO<sub>2</sub> thin